BORON DOPING AND POROSITY ENHANCE PHOTOCATALYTIC ACTIVITY OF GRAPHITIC CARBON NITRIDE FOR DICLOFENAC REMOVAL

Nguyen Thuy Giang[1,2], Nguyen The Hung[1], Hoang Van Hung[3], Nguyen Manh Dung[4], Nguyen Thi Khanh Van[5], Nguyen Thi Hien Luong[6], Le Thi Thuy Linh[7], Do Thi Lan[1*]

[1]TNU - University of Agriculture and Forestry, [2]TNU - University of Medicine and Pharmacy
[3]Thai Nguyen University, [4]Hanoi University of Natural Resources and Environment, [5]TNU - University of Sciences
[6]Huyen Anh Education and Study Abroad Co., LTD, [7]Phu Luong Agricultural Service Center, Thai Nguyen

ARTICLE INFO

Received: 27/8/2024
Revised: 03/12/2024
Published: 03/12/2024

KEYWORDS

Supramolecular self-assembly
Graphitic carbon nitride (g-C_3N_4)
Diclofenac (DCF)
Photocatalyst
Visible light

ABSTRACT

Wastewater contains trace amounts of antibiotics and dye, which can harm ecosystems and human health. This study presents a novel photocatalyst, boron-doped graphitic carbon nitride (B-g-C_3N_4), as a potential solution. Developed through two steps using hydrothermal self-assembly and thermal polymerization, B-g-C_3N_4 exhibits a distinctive tubular structure. The unique tubular structure remarkably increases its surface area and optical absorption, effectively degrading DCF under visible light. Compared to pure g-C_3N_4, the B-g-C_3N_4 material has a slightly increased surface area (from 14.83 to 16.47 m^2 g^{-1}). Moreover, the incorporation of boron into the g-C_3N_4 matrix narrows the energy band gap from 2.74 eV to 2.67 eV, allowing the B-g-C_3N_4 to absorb more effectively in the visible light region. As a result, more electron-hole pairs are generated, effectively initiating the photocatalytic degradation process. As a result, B-g-C_3N_4 exhibits remarkable efficiency in degrading DCF, achieving nearly 99% elimination in 60 min under visible light illumination. The outcome emphasizes the potential of B-g-C_3N_4 as a promising choice for environmental remediation applications.

TĂNG CƯỜNG HOẠT TÍNH QUANG XÚC TÁC CỦA GRAPHITIC CARBON NITRIDE BẰNG PHƯƠNG PHÁP PHA TẠP BORON VÀ TĂNG ĐỘ XỐP ĐỂ LOẠI BỎ DICLOFENAC

Nguyễn Thùy Giang[1,2], Nguyễn Thế Hùng[1], Hoàng Văn Hùng[3], Nguyễn Mạnh Dũng[4], Nguyễn Thị Khánh Vân[5], Nguyễn Thị Hiền Lương[6], Lê Thị Thùy Linh[7], Đỗ Thị Lan[1*]

[1]Trường Đại học Nông Lâm - ĐH Thái Nguyên, [2]Trường Đại học Y Dược - ĐH Thái Nguyên, [3]Đại học Thái Nguyên
[4]Trường Đại học Tài nguyên và Môi trường Hà Nội, [5]Trường Đại học Khoa học - ĐH Thái Nguyên,
[6]Công ty TNHH Giáo dục và Du học Huyền Anh, [7]Trung tâm Dịch vụ nông nghiệp huyện Phú Lương, Thái Nguyên

THÔNG TIN BÀI BÁO

Ngày nhận bài: 27/8/2024
Ngày hoàn thiện: 03/12/2024
Ngày đăng: 03/12/2024

TỪ KHÓA

Tự lắp ráp siêu phân tử
Graphitic carbon nitride (g-C_3N_4)
Diclofenac (DCF)
Chất xúc tác quang
Ánh sáng khả kiến

TÓM TẮT

Dư lượng kháng sinh và chất nhuộm trong nước thải tiềm ẩn nguy cơ gây hại cho hệ sinh thái và sức khỏe con người. Nghiên cứu này đã tìm ra một giải pháp với chất xúc tác quang mới là vật liệu g-C_3N_4 pha tạp boron (B-g-C_3N_4). Thông qua hai phương pháp tự lắp ráp thủy nhiệt và trùng hợp nhiệt, nghiên cứu đã tạo ra một vật liệu với cấu trúc ống nano độc đáo. Cấu trúc này không chỉ tăng đáng kể diện tích bề mặt mà còn tạo ra nhiều tâm hoạt động, giúp tăng cường khả năng hấp thụ ánh sáng và xúc tác quang phân hủy DCF dưới ánh sáng nhìn thấy. So với g-C_3N_4 không pha tạp, vật liệu B-g-C_3N_4 cho thấy sự tăng nhẹ diện tích bề mặt từ 14,83 đến 16,47 m^2 g^{-1}, góp phần tăng cường khả năng hấp phụ và xúc tác. Hơn nữa, việc pha tạp boron vào cấu trúc g-C_3N_4 thu hẹp khoảng trống năng lượng, từ 2,74 eV xuống 2,67 eV, cho phép vật liệu hấp thụ hiệu quả hơn trong vùng ánh sáng nhìn thấy. Kết quả là, nhiều cặp electron-lỗ trống được tạo ra, góp phần tăng hiệu quả quá trình phân hủy quang xúc tác. Do đó, B-g-C_3N_4 thể hiện hiệu quả đáng kể trong việc phân hủy DCF, đạt gần 99% loại bỏ trong 60 phút dưới chiếu sáng của ánh sáng nhìn thấy. Kết quả nhấn mạnh tiềm năng của g-C_3N_4 như một lựa chọn hiệu quả cho các ứng dụng phục hồi môi trường.

DOI: https://doi.org/10.34238/tnu-jst.11013

* Corresponding author. *Email: dothilan@tuaf.edu.vn*

1. Introduction

In recent decades, urbanization and population growth have led to a significant rise in environmental pollution. Wastewater often contains trace amounts of diclofenac (DCF), a common antibiotic found at concentrations ranging from nanograms to micrograms per liter. Despite its low levels, DCF can significantly affect public health and the environment [1]. It can damage habitats, reduce the biodiversity of aquatic species, and contribute to the development of antibiotic-resistant bacteria, which can infect humans through the food supply [2] - [4]. Traditional wastewater treatment methods such as adsorption biological processes, and electrochemical oxidation often prove ineffective in removing antibiotics due to low removal rates, complex procedures, and high costs. Therefore, developing more advanced and sustainable wastewater treatment methods is urgently needed.

Currently, photocatalytic technology based on semiconductors is considered the most environmentally friendly and optimal solution among all possible options. It has been rapidly gaining popularity worldwide due to its environmentally friendly properties. Graphite carbon nitride (g-C_3N_4) has high photocatalytic activity, allowing it to convert solar energy into chemical energy, making it an ideal photocatalyst for various applications [5]. Moreover, g-C_3N_4 is an attractive choice since it is inexpensive, readily available, and non-toxic. It has proven an effective and eco-friendly alternative to traditional photocatalytic materials such as TiO_2, CdS, and ZnO [6]. Due to its versatile properties, g-C_3N_4 holds great promise for many applications, including solar energy conversion and wastewater treatment. However, the weak catalytic activity of g-C_3N_4 imposes limitations on its applications due to low specific surface area and high recombination rate of photogenerated electron-hole pairs.

One effective strategy to address this limitation is non-metal doping into g-C_3N_4, which allows for the introduction of additional energy levels, which can also increase the rate of charge separation [7]. The modifications can help to improve the photocatalytic efficiency of g-C_3N_4. For example, doping different elements such as F, P, O can increase the absorption of visible light, effective in improving its photocatalytic efficiency. Due to the introduction of impurities, element-doped g-C_3N_4 can exhibit enhanced visible light absorption and photocatalytic activity [7], [8]. Moreover, the morphology control has the advantage of helping to control the size and shape of material, which in turn influences the amount of incident light that can be absorbed. Hollow porous structures are particularly promising, as it can reduce the charge and mass diffusion lengths resulting in more efficient photocatalysis [9]. Recently, the supramolecular preorganization strategy has been promising for creating nanoporous tubular materials with tailored pore sizes and structures. Due to the directionality and saturability of hydrogen bonds, the as-grown supramolecular precursors usually possess ordered structures. Moreover, the aqueous environment of the supramolecular self-assembly process does not require harsh reaction conditions, which can damage the environment or create impurities, and it is also much safer than other methods [10].

This study successfully developed the tubular B-doped g-C_3N_4 using melamine, cyanuric acid, and boric acid as precursors. The B-g-C_3N_4 was characterized through X-ray diffraction (XRD), scanning electron microscopy (SEM), and Brunauer-Emmett-Teller (BET) analysis. The optical properties and band gap were analyzed using diffuse reflectance spectroscopy (DRS). Scavenger experiments and electron paramagnetic resonance (EPR) techniques were conducted to detect the primary radical species involved. A plausible photodegradation mechanism for DCF was proposed based on the findings. Overall, the synthesized material exhibited a desirable morphology, positioning it as a promising candidate for real-world applications.

2. Experimental section

2.1. Chemical reagents

Melamine and diclofenac (DCF) were obtained from Merck, while p-benzoquinone (BQ), ammonium oxalate (AO), boric acid, 5,5-dimethyl-1-pyrroline (DMPO), and 2,2,6,6-tetramethylpiperidine (TEMP) were supplied by Sigma-Aldrich. Various analytical chemicals were acquired for the study, and no additional purification was performed. Milli-Q ultrapure water with a resistivity of 18.2 MΩ cm was utilized to prepare all solutions.

2.2. Synthesis of g-C_3N_4 and B-doped g-C_3N_4

A two-step hydrothermal and thermal polymerization method was utilized to synthesize g-C_3N_4 and B-doped g-C_3N_4. In this procedure, equal molar ratios of melamine and cyanuric acid were individually dispersed in 100 mL of DI water at 80°C until completely dissolved. Subsequently, boric acid was added and vigorously stirred. The resulting mixtures were combined and transferred into a Teflon-lined tube, then heated to 160°C for 12 hours. After cooling to room temperature, the white solution underwent filtration, followed by washing with deionized water and ethanol. The resulting material was dried at 60°C and ground into a powder. The powder was then placed in a crucible with a lid and calcined at 550°C for 4 hours, using a ramp rate of 2°C/min to obtain boron-doped g-C_3N_4 (B-g-C_3N_4). For comparison, pure g-C_3N_4 was synthesized using the same experimental steps but without adding boric acid.

2.3. Photocatalytic experiments

The prepared catalysts (1 g/L) were added to a DCF solution (100 mL, 5 mg/L) at 25°C and continuously stirred in the dark for 30 minutes to evaluate the activity. Afterward, the photocatalysts were exposed to continuous illumination from a 300W Xenon lamp (with a UV cut-off filter) to initiate the photocatalytic degradation process. A 2 mL sample was withdrawn and centrifuged at intervals, and the supernatant was used for further analysis. DCF concentrations in the filtrate were determined using HPLC with a C-18 column (Phenomenex, 5 μm, 4.6 mm × 250 mm). A mobile phase of acetonitrile/phosphate buffer (70:30, v/v) was used at 1 mL/min, and absorbance was measured at 276 nm. Additionally, p-benzoquinone (pBQ), isopropanol (IPA), and ammonium oxalate (AO) were added to the DCF solution as scavengers for superoxide anion ($O_2^{\bullet-}$), hydroxyl radical ($OH^{\bullet}$), and hole (h^+), respectively, to quench photoactivity.

2.4. Material characterization

XRD analysis of the as-prepared samples was performed on a Bruker D8 Advance diffractometer using Cu Kα radiation (λ = 1.5406 Å) at 40 kV and 40 mA, scanning from 10° to 60°. FTIR spectroscopy characterized functional groups (400-4000 cm^{-1}), while DRS used UV-Vis to investigate the optical properties. BET analysis determined specific surface area, and SEM imaging examined morphology and microstructure using a microscope.

3. Results and discussion

3.1. Characterization of materials

To study the morphology of the as-prepared photocatalyst, SEM was employed (Figure 1a, b). Notably, the g-C_3N_4 and B-g-C_3N_4 samples exhibited tubular structure, with lengths spanning several μm and diameters of approximately 5 μm. The observation suggests that the introduction of the B element did not significantly affect the microstructure of the material. The hydrothermal treatment initiated the formation of a supramolecular complex between cyanuric acid and melamine. The strong electrostatic interaction between melamine molecules facilitated the formation of hydrogen bonds, resulting in the self-assembly of the molecules into a hollow

porous shape [8]. The structure provides an advantageous environment for catalytic reactions as it facilitates the interaction between the concentration of reactants and the catalytic sites on the material, thereby promoting efficient reactant-catalyst interactions.

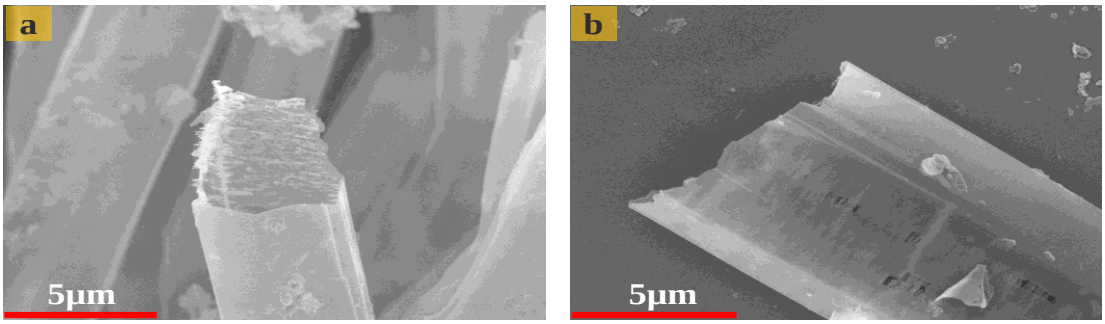

Figure 1. *SEM images of porous (a) g-C_3N_4 and (b) B-g-C_3N_4*

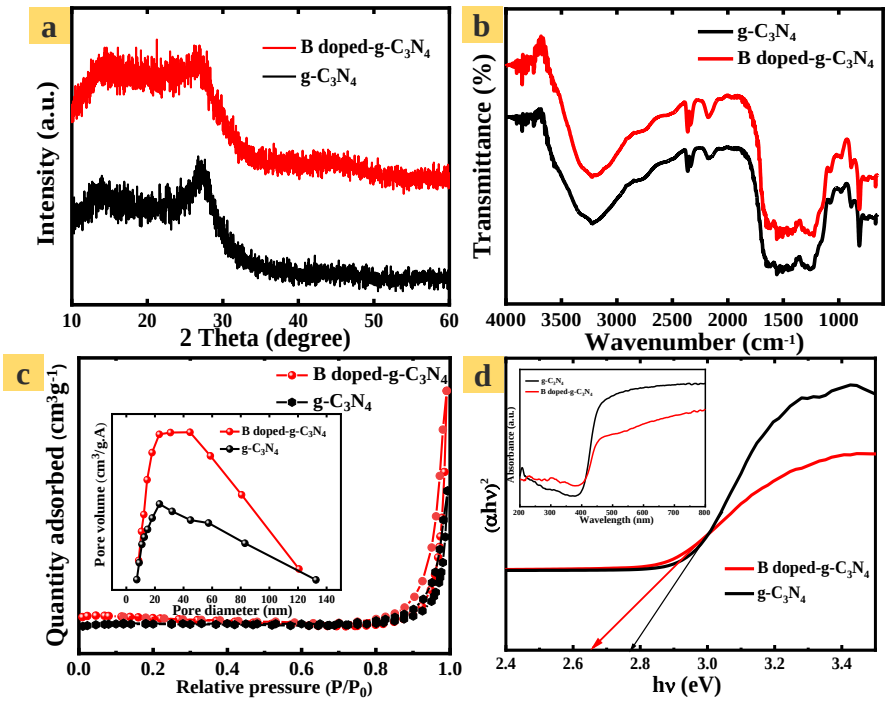

Figure 2. *(a) XRD patterns, (b) FTIR, (c) BET and pore size distribution, and (d) the UV-Vis diffuse reflectance spectroscopy (DRS) and bandgaps of g-C_3N_4 and B-g-C_3N_4*

The crystal structure and phases in the as-synthesized samples were analyzed using X-ray diffraction (XRD) patterns (Figure 2a). The presence of two characteristic peaks in the XRD pattern confirmed the crystalline structure of g-C_3N_4. The (100) peak is indicative of the crystalline structure of the tris-s-triazine unit at around 13.2° 2θ, while the (002) peak is indicative of the stacking of conjugated aromatic planes at around 27.2° 2θ [7]. X-ray diffraction analysis showed no significant change in the crystal lattice of the B-g-C_3N_4, which suggests that the basic structure of the g-C_3N_4 was maintained.

FTIR provides further insight into the chemical composition and bonding structure via the vibrational frequencies of molecules of the materials (Figure 2b). The presence of a small and sharp peak at 800 cm^{-1} is indicative of the breathing mode of tri-s-triazine units in the molecule, and the broadband in the range of 1200 - 1700 cm^{-1} was assigned to the bending vibrations of

conjugated C–N, C=N heterocycles. Furthermore, the broad peak at 3000–3400 cm^{-1} was assigned O–H groups [5]. It is important to note that the detection of boron-related peaks was insignificant which suggests that the sample may contain a very low boron content, making it more difficult to detect.

As shown in Figure 2c, B-g-C_3N_4 demonstrates a larger BET surface area (16.47 m^2 g^{-1}) than the bulk g-C_3N_4 (14.83 m^2 g^{-1}). Moreover, the photocatalysts exhibit a wide range of pore sizes, typically 10 to 140 nm, with a predominant mesoporous structure characterized by a pore size distribution from 10 to 60 nm. The hollow porous configuration of the materials, combined with a hierarchical pore structure derived from supramolecular precursors, plays a vital role in active sites for photocatalytic reactions.

UV-vis diffuse reflectance spectroscopy is a technique utilized to measure the light absorption of materials. In Figure 2d, it can be observed that all samples exhibit significant absorption in the visible range. Compared to pure g-C_3N_4, B-g-C_3N_4 demonstrates a redshift around 460 nm, indicating that boron doping significantly enhances the light absorption properties by incorporating boron atoms at the absorption edge. Modifying the electronic structure and decreasing the band gap of B-g-C_3N_4 resulted in a red shift in the absorption spectrum. The calculated Eg values for g-C_3N_4 and B-g-C_3N_4 were 2.78 and 2.67 eV, respectively. The incorporation of the boron dopant enhances the ability of B-g-C_3N_4 to absorb light, leading to an improved capacity for generating photogenerated electron (e^-) and hole (h^+) species. Additionally, the porous structure of g-C_3N_4 further contributes to its light absorption ability by facilitating multiple reflections of incident light [10].

3.2. Photocatalytic performance evaluation

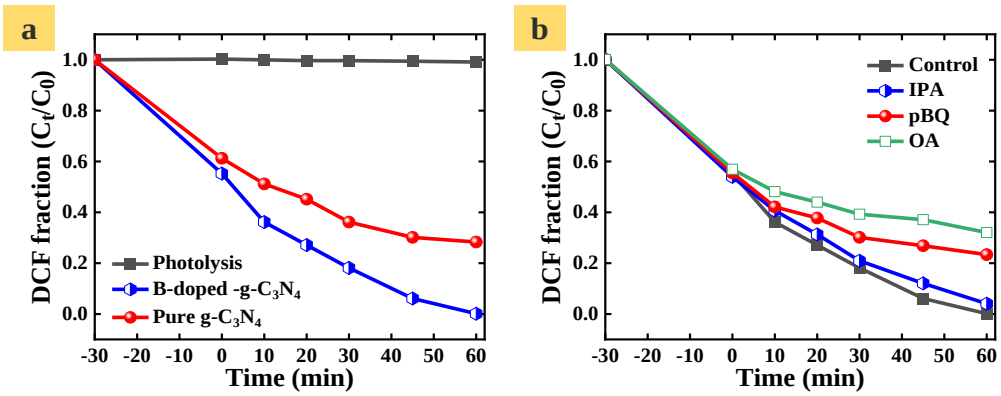

Figure 3. *(a) The photocatalytic degradation of DCF of g-C_3N_4 and B-g-C_3N_4 and (b) Radicals (h^+, $O_2^{\bullet -}$ and $OH^{\bullet}$) capture experiments using AO, pBQ and IPA over B-g-C_3N_4 Conditions: [phocatalyst] = 1 g/L, [DCF] = 10 mg/L, pH = 7, T = 25°C*

The photocatalyst achieved its dark adsorption equilibrium prior to being exposed to visible light, as illustrated in Figure 3a. The adsorption of DCF demonstrated moderate efficacy, between 38 and 44% of the contaminant within 30 min. Consequently, additional treatment was necessary to achieve complete contaminant elimination. Nevertheless, the incorporation of photocatalysis substantially improved the removal of DCF. As a result, g-C_3N_4 obtained a 72% removal rate after 60 min of light exposure, while B-doped g-C_3N_4 exhibited exceptional efficacy, achieving a 99% removal rate. It is important to note that the concentration of DCF did not diminish over time in the time-dependent experiments, which implies that self-degradation is not a significant factor. The result underscores the critical role of boron doping in the g-C_3N_4 network in the photocatalytic degradation of DCF. The boron-doped g-C_3N_4 leads to a decrease in the band gap, which enhances the utilization of light adsorption. Additionally, the hollow

porous structure maximizes light absorption and enhances effective chemical reactions, significantly improving its photocatalytic efficiency.

Radical trapping and EPR experiments are conducted to detect the generation of reactive oxygen species. As shown in Figure 3b, in the presence of IPA, degradation efficiency decreases to 95%, followed by 76% and 68% following the addition of pBQ and AO, respectively [10]. The result indicates that superoxide anion ($O_2^{\bullet-}$) and hole (h^+) radicals are the main causes of DCF oxidation. Moreover, EPR spectroscopy was used to measure the formation of $OH^{\bullet}$ and $O_2^{\bullet-}$species in both dark and visible light irradiation conditions.

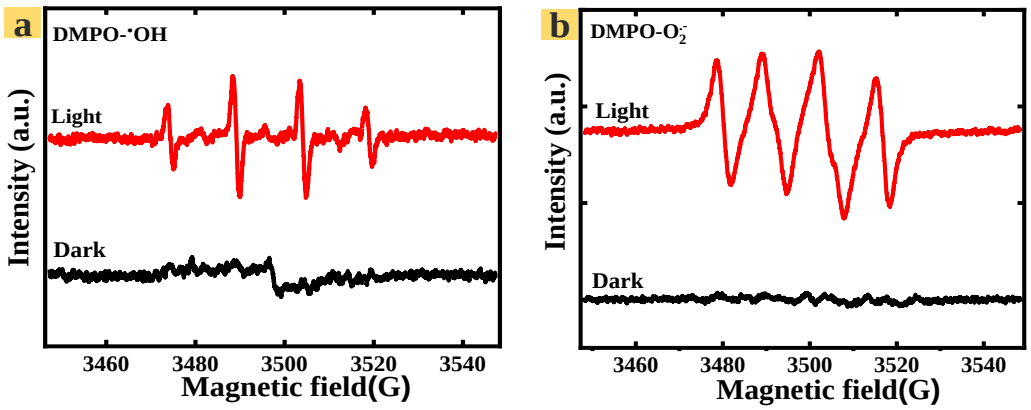

Figure 4. *(a) The EPR signals of DMPO-$OH^{\bullet}$ and (b)DMPO-$O_2^{\bullet-}$ in the dark and under visible light irradiation over B-g-C_3N_4*

Figure 4 (a, b) shows that the signal peaks of DMPO-$OH^{\bullet}$ and DMPO-$O_2^{\bullet-}$ are rarely observed in the dark. However, light irradiation enhances the intensity of both DMPO-$O_2^{\bullet-}$ and DMPO-$OH^{\bullet}$ peaks. The result strongly indicates the importance of oxygen-containing radicals in the degradation of DCF under visible light.

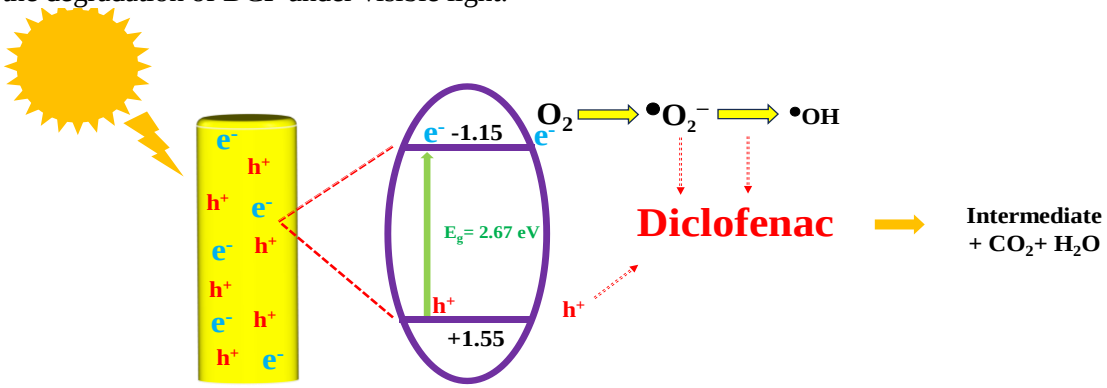

Figure 5. *The mechanism diagram of the photocatalytic degradation of DCF over B-g-C_3N_4*

Based on the experimental results reported above, a possible DCF photodegradation mechanism over B-g-C_3N_4 under visible light was proposed in Figure 5. Upon activation by the photons of the light, B-g-C_3N_4 undergoes excitation, generating the photogenerated electrons in the conduction band (CB) and holes in the valence band (VB). Due to the more negative conduction band potential of B-g-C_3N_4 compared to the reduction potential of $O_2/O_2^{\bullet-}$ (-0.32 eV), the photoinduced electrons can effectively reduce dissolved O_2, resulting in the formation of $O_2^{\bullet-}$radicals. The $O_2^{\bullet-}$ radicals can further react to produce hydrogen peroxide (H_2O_2) and subsequently generate hydroxyl radicals (•OH). However, the valence band (VB) of B-g-C_3N_4 is more negative than the standard redox potential of •OH /OH^-. Therefore, the holes are unable to oxidize OH- into $^{\bullet}$OH; meanwhile, h^+ can directly oxidize DCF. As a result, ROS, including

$O_2^{\bullet-}$, $OH^{\bullet}$, and h^+, generated during the photocatalytic process can effectively oxidize organic pollutants into harmless compounds such as CO_2 and water [8], [10].

$$B\text{-}g\text{-}C_3N_4 + h\upsilon \rightarrow h^+ + e^- \quad (1)$$

$$e^- + O_2 \rightarrow O_2^{\bullet-} \quad (2)$$

$$O_2^{\bullet-} + H^+ \rightarrow \bullet OOH \quad (3)$$

$$\bullet OOH + H^+ + e^- \rightarrow H_2O_2 \quad (4)$$

$$H_2O_2 + e^- \rightarrow OH^{\bullet} + OH^- \quad (5)$$

$$O_2^{\bullet-}, h^+, OH^{\bullet} + DCF \rightarrow \text{Degraded or mineralized products} + CO_2 \text{ and } H_2O \quad (6)$$

4. Conclusion

In this study, we successfully synthesized boron-doped porous g-C_3N_4 through hydrothermal and thermal polymerization methods. The hollow porous morphology was advantageous, allowing for multiple refractions of incident light within the tube walls, thereby maximizing light conversion efficiency. Moreover, boron doping improved the separation efficiency of h^+-e^- pairs by acting as an electron acceptor and helping to reduce the band gap. As a result, the B-g-C_3N_4 exhibited excellent visible light photocatalytic efficiency in DCF degradation at 99% in 60 minutes. The dominant species involved in DCF degradation were $O_2^{\bullet-}$and h^+. The advantages of the B-g-C_3N_4 show the rational design of photocatalysts, enabling the versatile application of B-doped g-C_3N_4 in wastewater treatment and solar energy conversion.

Acknowledgments

The authors thank the Vietnam Ministry of Education and Training for the financial support provided under grant number B2023-TNA-23.

REFERENCES

[1] P. Mathur, D. Sanyal, D. L. Callahan, X. A. Conlan, and F. M. Pfeffer, "Treatment technologies to mitigate the harmful effects of recalcitrant fluoroquinolone antibiotics on the environ-ment and human health," *Environ. Pollut.*, vol. 291, 2021, Art. no. 118233.

[2] A. Monteoliva-García, J. Martín-Pascual, M. D. M. Muñío, and J. M. Poyatos, "Effects of carrier addition on water quality and pharmaceutical removal capacity of a membrane bioreactor–advanced oxidation process combined treatment," *Sci. Total Environ.*, vol. 708, 2020, Art. no. 135104.

[3] S. Bhatt and S. Chatterjee, "Fluoroquinolone antibiotics: Occurrence, mode of action, resistance, environmental detection, and remediation–A comprehensive review," *Environ. Pollut.*, vol. 315, 2022, Art. no. 120440.

[4] F. Guo, H. Zhang, H. Li, and Z. Shen, "Modulating the oxidative active species by regulating the valence of palladium cocatalyst in photocatalytic degradation of ciprofloxacin," *Appl. Catal.*, vol. 306, 2022, Art. no. 121092.

[5] J. Fu, J. Yu, C. Jiang, and B. Cheng, "g-C_3N_4-Based heterostructured photocatalysts," *Adv. Energy Mater.*, vol. 8, no. 3, 2018, Art. no. 1701503.

[6] L. Chen, M. A. Maigbay, M. Li, and X. Qiu, "Synthesis and modification strategies of g-C_3N_4 nanosheets for photocatalytic applications," *Appl. Mater. Today*, vol. 3, no. 1, 2023, Art. no. 100150.

[7] V. Hasija *et al.*, "Oxygen doping facilitated N-vacancies in g-C_3N_4 regulates electronic band gap structure for trimethoprim and Cr (VI) mitigation: simulation studies and photocatalytic degradation pathways," *Appl. Mater. Today*, vol. 29, 2022, Art. no. 101676.

[8] M. D. Nguyen, T. B. Nguyen, A. Thamilselvan, T. G. Nguyen, E. P. Kuncoro, and R.-A. Doong, "Fabrication of visible-light-driven tubular F, P-codoped graphitic carbon nitride for enhanced photocatalytic degradation of tetracycline," *J. Environ. Chem. Eng.*, vol. 10, no. 1, 2022, Art. no. 106905.

[9] F. Chen, L. L. Liu, J. H. Wu, X. H. Rui, J. J. Chen, and Y. Yu, "Single-Atom Iron Anchored Tubularg-C_3N_4 Catalysts for Ultrafast Fenton-Like Reaction: Roles of High-Valency Iron-Oxo Species and Organic Radicals," *Adv. Mater.*, vol. 34, no. 31, 2022, Art. no. 2202891.

[10] J. Xing *et al.*, "N-doped synergistic porous thin-walled g-C_3N_4 nanotubes for efficient tetracycline photodegradation," *Chemical Engineering Journal*, vol. 455, 2023, Art. no. 140570.